

Looking for Cosmological Alfvén Waves in WMAP Data

Gang Chen¹, Pia Mukherjee², Tina Kahniashvili^{1,3}, Bharat Ratra¹, and Yun Wang²

ABSTRACT

A primordial cosmological magnetic field induces and supports vorticity or Alfvén waves, which in turn generate cosmic microwave background (CMB) anisotropies. A homogeneous primordial magnetic field with fixed direction induces correlations between the $a_{l-1,m}$ and $a_{l+1,m}$ multipole coefficients of the CMB temperature anisotropy field. We discuss the constraints that can be placed on the strength of such a primordial magnetic field using CMB anisotropy data from the WMAP experiment. We place 3σ upper limits on the strength of the magnetic field of $B < 15$ nG for vector perturbation spectral index $n = -5$ and $B < 1.7$ nG for $n = -7$.

Subject headings: cosmic microwave background — cosmology: observation — methods: statistical

1. Introduction

The origin of the large-scale part of observed galactic magnetic fields, of $\sim \mu\text{G}$ (micro-Gauss) strength and apparently coherent over ~ 10 kpc scales, is unknown. They could be the consequence of nonlinear amplification of a tiny seed field by galactic dynamo processes. An alternate possibility is amplification of a weak seed field through anisotropic protogalactic collapse and subsequent further amplification via galactic differential rotation. In both cases a primordial seed field of strength exceeding 10^{-13} to 10^{-12} G, coherent over $\sim \text{Mpc}$ scales, is apparently needed, and it is often suggested that upto a $\sim \text{nG}$ strength seed field

¹Department of Physics, Kansas State University, 116 Cardwell Hall, Manhattan, KS 66506.

²Department of Physics and Astronomy, University of Oklahoma, 440 W. Brooks Street, Norman, OK 73019.

³Center for Plasma Astrophysics, Abastumani Astrophysical Observatory, A. Kazbegi ave 2a, Tbilisi, 380060, Republic of Georgia.

might be required. See Kulsrud (1999), Widrow (2002), and Giovannini (2003) for reviews of the state of the art in this area. A primordial magnetic field of present strength \sim nG can leave observable signatures in the cosmic microwave background (CMB) anisotropy.

In standard cosmologies vorticity perturbations decay and so do not contribute to CMB temperature or polarization anisotropies. The presence of a cosmological magnetic field generated during an earlier epoch¹ changes this situation: a primordial magnetic field induces and supports vorticity or Alfvén waves (Adams et al. 1996; Durrer, Kahniashvili, & Yates 1998, hereafter DKY). These vector perturbations generate CMB anisotropies.² The presence of a preferred direction due to a homogeneous magnetic field background leads to an m dependence of $\langle a_{lm} a_{lm}^* \rangle$, and induces correlations between the $a_{l+1,m}$ and $a_{l-1,m}$ multipole coefficients of the CMB temperature anisotropy field. Since the CMB anisotropies are observed to be random Gaussian³, it is known that such a contribution can only be subdominant.

We use the observed $\overline{\langle a_{l-1,m} a_{l+1,m}^* \rangle}$ correlations measured by WMAP to place constraints on the strength of a homogeneous primordial magnetic field. The angular brackets here denote an ensemble average, and the overbar indicates an average over m for each l . Limited by cosmic variance uncertainties, this would be the useful measure to characterize the signature of a homogeneous primordial magnetic field.

¹Quantum fluctuations during an early epoch of inflation can generate a primordial nG magnetic field, coherent over very large scales (see, e.g., Ratra 1992; Bamba & Yokoyama 2004)

²In the future one can hope to constrain vector modes through their effect on CMB anisotropy polarization anisotropy spectra. CMB polarization spectra that result from vector perturbations due to a primordial magnetic field have been discussed by Seshadri & Subramanian (2001), Pogosian, Vachaspati, & Winitzki (2002), Mack, Kahniashvili, & Kosowsky (2002), and Subramanian, Seshadri, & Barrow (2003), while Lewis (2004) considers the case of vector modes supported by free-streaming neutrinos.

³Colley, Gott, & Park (1996), Mukherjee, Hobson, & Lasenby (2000), and Park et al. (2001) are some early discussions of the Gaussianity of the CMB anisotropy. More recent discussions of the Gaussianity of the WMAP CMB anisotropy data are in Komatsu et al. (2003), Colley & Gott (2003), Chiang et al. (2003), Park (2004), Eriksen et al. (2004a, 2004b), Coles et al. (2004), Vielva et al. (2004), Copi, Huterer, & Starkman (2003), Hansen et al. (2004), Gurzadyan et al. (2004), and Mukherjee & Wang (2004). The simplest inflation models predict Gaussian fluctuations (see, e.g., Fischler, Ratra, & Susskind 1985; Ratra 1985), and this is consistent with most observational indications (see, e.g., Peebles & Ratra 2003). While there are indications of mild peculiarities in some subsets of the WMAP data, for example the apparent paucity of large-scale power (Spergel et al. 2003; see Górski et al. 1998a for a similar indication from COBE data) and the differences between data from different parts of the sky (see papers cited above), foreground contamination (see, e.g., Park, Park, & Ratra 2002; Mukherjee et al. 2002, 2003; de Oliveira-Costa et al. 2003; Bennett et al. 2003b; Tegmark, de Oliveira-Costa, & Hamilton 2003) and other systematics might be responsible for part of this.

The model on which we base our analysis is introduced in §2. Our analysis of the WMAP data and our results are discussed in §3. We conclude in §4.

2. CMB temperature anisotropies generated by Alfvén waves

We assume that the homogeneous magnetic field \mathbf{B} is generated prior to the time of recombination. Such a field could be generated during the electroweak phase transition (see, e.g., Vachaspati 1991; Sigl, Olinto, & Jedamzik 1997; Giovaninni & Shaposhnikov 1998), or by an α -effect dynamo driven by collective neutrino-plasma interactions (Semikoz & Sokoloff 2004). The energy density of this field, $B^2/(4\pi)$, must be small, to prevent a violation of the cosmological principle, and so may be treated as a first order perturbation. Accounting for the high conductivity of the primordial non-relativistic plasma (with $v \ll 1$ where \mathbf{v} is the velocity field of the plasma), we may use the infinite conductivity, frozen-in condition, $\mathbf{E} + \mathbf{v} \times \mathbf{B} = 0$. We also assume that charged particles are tightly coupled to the radiation. We write $\mathbf{B} = \mathbf{B}_0 + \mathbf{B}_1$, where \mathbf{B}_1 denotes the first order vector perturbation in the magnetic field (where $\nabla \cdot \mathbf{B}_1 = 0$), and $\mathbf{v} = 0 + \mathbf{\Omega}$ with $\mathbf{\Omega}$ being the first order vector perturbation in the fluid velocity (where $\nabla \cdot \mathbf{\Omega} = 0$).

As a consequence of magnetic flux conservation the field lines in an expanding universe are conformally diluted, $B_0 \propto 1/a^2$, and the Alfvén velocity in the photon-baryon plasma during the photon dominated epoch when the energy density $\rho_R = \rho_\gamma + \rho_b \simeq \rho_\gamma$ until recombination, is $v_A = B_0/\sqrt{4\pi(\rho_R + p_R)} = 4 \times 10^{-4}(B_0/10^{-9}\text{G})$, and is time independent. Rescaling physical quantities according to the expansion of the universe, the MHD equations result in an equation describing Alfvén wave propagation with velocity $v_A(\mathbf{b} \cdot \hat{\mathbf{k}}) \equiv v_A\mu$ (DKY)

$$\ddot{\mathbf{\Omega}} = v_A^2(\mathbf{b} \cdot \mathbf{k})^2\mathbf{\Omega}. \quad (1)$$

Here $\mathbf{b} \equiv \mathbf{B}_0/B_0$ is the unit vector in the direction of the magnetic field and an overdot denotes a derivative with respect to conformal time η . Choosing only the sine mode, to satisfy the initial condition $\mathbf{\Omega}(\mathbf{k}, \eta = 0) = 0$, we have

$$\mathbf{\Omega}(\mathbf{k}, \eta) \simeq \mathbf{\Omega}_0 v_A k \mu \eta, \quad |\mathbf{\Omega}_0| = \frac{v_A}{B_0} |\mathbf{B}_1|. \quad (2)$$

In eq. (1) we have neglected viscosity so the vorticity solution in eq. (2) is applicable only on scales bigger than the damping scale. Assuming that the initial vector perturbation is generated by a random process, the two-point correlation function of the vorticity field can be written as (Pogosian et al. 2002)

$$\langle \Omega_{0i}^*(\mathbf{k}) \Omega_{0j}(\mathbf{k}') \rangle = \left[(\delta_{ij} - \hat{k}_i \hat{k}_j) S(k) + i \epsilon_{ijl} \hat{k}_l A(k) \right] \delta(\mathbf{k} - \mathbf{k}'). \quad (3)$$

Here ϵ_{ijl} is the totally antisymmetric tensor, and the $S(k)$ and $A(k)$ power spectra describe the symmetric and helical parts of the two-point correlation function. We assume that the spectra $S(k)$ ($= |\Omega_0(k)|^2$) and $A(k)$ are given by simple power laws of the scale $1/k$ on scales larger than the perturbation damping scale $1/k_D$, i.e., for $k < k_D$ we take $S(k) = S_0 k^n / k_D^{n+3}$ and $A(k) = A_0 k^m / k_D^{m+4}$. Here S_0 and A_0 are dimensionless normalization constants with $S_0 \geq A_0$, and n and m are spectral indexes. The cutoff scale $1/k_D$ is the scale below which the magnetic field is damped away, due to the non-infinite value of the conductivity. Using $T_{\text{dec}} \sim 0.3 \text{ eV}$ and $t_{\text{dec}} \sim 10^{23} \text{ cm}$, the comoving magnetic field damping wave number at decoupling is $k_D(t = t_{\text{dec}}) \sim 3 \times 10^{-10} \text{ cm}^{-1}$ (DKY).

The CMB fractional temperature anisotropy, in direction \mathbf{n} on the sky, induced by a vorticity perturbation (ignoring a possible dipole contribution from the vector perturbation) is (DKY)

$$\frac{\Delta T}{T}(\mathbf{n}, \mathbf{k}) \simeq \mathbf{n} \cdot \boldsymbol{\Omega}(\mathbf{k}, \eta) = \mathbf{n} \cdot \boldsymbol{\Omega}_0 v_A \mu(k \eta_{\text{dec}}). \quad (4)$$

Decomposing the CMB fractional temperature anisotropy in a spherical harmonic expansion,

$$\frac{\Delta T}{T}(\mathbf{n}) = \sum_{l=2}^{\infty} \sum_{m=-l}^l a_{lm} Y_{lm}(\mathbf{n}) \quad (5)$$

and using the definition of the power spectrum C_l ,

$$\left\langle \frac{\Delta T}{T}(\mathbf{n}) \frac{\Delta T}{T}(\mathbf{n}') \right\rangle = \frac{1}{4\pi} \sum_{l=2}^{\infty} (2l+1) C_l P_l(\mathbf{n} \cdot \mathbf{n}'), \quad (6)$$

where P_l is the Legendre polynomial, we obtain, in the isotropic case, $C_l = \langle a_{lm}^* a_{lm} \rangle$. Here the angular brackets denote a theoretical (averaging) expectation value over an ensemble of statistically identical universes. In Fourier space this expectation value can be replaced by integration over all possible wavenumbers, i.e., $\langle \dots \rangle \rightarrow \int d^3 \mathbf{k} / (2\pi)^3$.

Computing $\langle a_{lm}^* a_{l'm'} \rangle$, it can be shown that the helical part of vorticity does not contribute (see Pogosian et al. 2002). Hence in what follows we consider only the symmetric part of the spectrum. Detailed computation of C_l 's for vorticity perturbations are described in DKY where it has been shown that the presence of a homogeneous magnetic field induces off-diagonal correlations in multipole space, in particular correlations between l and $l \pm 2$ multipole coefficients. To quantify this we introduce a second power spectrum defined by

$$D_l(m) = \langle a_{l-1,m}^* a_{l+1,m} \rangle = \langle a_{l+1,m}^* a_{l-1,m} \rangle. \quad (7)$$

The two power spectra, $C_l(m)$ and $D_l(m)$, depend on the spectral index n , the normalization constant S_0 , the Alfvén velocity v_A and the perturbation damping wavenumber k_D . The

power spectra are defined only for $n > -7$ (the quadrupole diverges at small k for $n \leq -7$), and for $n > -1$ the results are determined by the damping wavenumber k_D . The case $n = -5$ corresponds to the Harrison-Peebles-Yu-Zel’dovich scale-invariant spectrum ($C_l, D_l \sim l^2$). See DKY for a more detailed discussion.

The non-zero correlation of temperature for unequal l ’s has a simple physical explanation: The presence of a preferred spatial direction, that of the magnetic field \mathbf{B}_0 , breaks the spatial isotropy of the CMB map, leading not only to an m dependence of the correlators, but also non-zero off-diagonal (in l space) correlations.⁴ The temperature perturbation correlation between two points on the sky depends not only on the angular separation between the two points, but also on their orientation with respect to the magnetic field.

A simple observational test to detect (or constrain) the presence of a homogeneous magnetic field in the Universe is based on computing the D_l spectrum of CMB anisotropy data.⁵ For this it is useful to introduce the arithmetic mean over m of the two power spectra,

$$\begin{aligned}\bar{C}_l &\equiv \overline{\langle a_{lm}^* a_{lm} \rangle} = \frac{1}{2l+1} \sum_{m=-l}^l \langle a_{lm}^* a_{lm} \rangle \\ \bar{D}_l &\equiv \overline{\langle a_{l-1,m}^* a_{l+1,m} \rangle} = \frac{1}{2l+1} \sum_{m=-l}^l \langle a_{l-1,m}^* a_{l+1,m} \rangle.\end{aligned}\quad (8)$$

According to DKY,

$$\bar{C}_l \simeq S_0 \left(\frac{\eta_{\text{dec}}}{\eta_0} \right)^2 (k_D \eta_0)^{-(n+3)} v_A^2 \frac{2^{n+1} \Gamma(-n-1)}{3\Gamma(-n/2)^2} l^{n+3}, \quad n < -1 \quad (9)$$

$$\bar{C}_l / \bar{D}_l = |n+1| \left[\frac{\Gamma(-\frac{n+1}{2})}{\Gamma(-\frac{n}{2})} \right]^2 \quad n < -1. \quad (10)$$

$$\bar{C}_l \simeq \bar{D}_l \simeq S_0 \left(\frac{\eta_{\text{dec}}}{\eta_0} \right)^2 (k_D \eta_0)^{-2} v_A^2 \frac{1}{n+1} l^2, \quad n > -1 \quad (11)$$

Using $\mathbf{B}_1 \leq \mathbf{B}_0$, we have $|\mathbf{\Omega}_0|^2 k^3 \leq v_A^2$ (see eq. [2]). This inequality must hold on all scales inside the Hubble radius at decoupling, $k \geq 1/\eta_{\text{dec}}$. With the $S(k)$ spectrum definition in eq. (3) we therefore get $2S_0(k/k_D)^{n+3} \leq v_A^2$ for $1/\eta_{\text{dec}} \leq k \leq k_D$, implying

$$2S_0(k_D \eta_{\text{dec}})^{-(n+3)} \leq v_A^2 \quad n \leq -3, \quad (12)$$

⁴In a recent paper, Bershadskii & Sreenivasan (2004) show that collisions between Alfvén wave packets and their cascades could generate arcminute-scale CMB temperature anisotropies, and argue that this is consistent with the WMAP data.

⁵Other statistics, related to the D_l ’s here, could also provide useful tests (e.g., Hajian & Souradeep 2003).

$$2S_0 \leq v_A^2 \quad n \geq -3. \quad (13)$$

So for $n \leq -3$ the result is independent of the damping wavenumber k_D .

We now estimate an upper limiting value of l , l_C , beyond which our approximation is no longer valid. Just like scalar perturbations (Peebles 1980), vector perturbations are affected by collisionless damping. Adding a photon drag force term on the right hand side of the vorticity equation (1), we can see that there are no oscillations in the vector perturbation case, and that damping occurs on scales slightly larger than the damping scale for scalar perturbations, when $k_C \eta_{\text{dec}} \sim 10$ (DKY), corresponding to $l_C \sim 500$, beyond which our approximation breaks down.

Inserting the limiting values given for S_0 in eqs. (12) and (13) in eq. (9), we find for $n = -5$,

$$\overline{C}_l = 9.04 \times 10^{-16} l^{-2} \left(\frac{B}{1 \text{ nG}} \right)^4, \quad \overline{D}_l = \overline{C}_l / 2.26, \quad (14)$$

and, for $n = -7$,

$$\overline{C}_l = 8.61 \times 10^{-10} l^{-4} \left(\frac{B}{1 \text{ nG}} \right)^4, \quad \overline{D}_l = \overline{C}_l / 2.17. \quad (15)$$

In this paper, we use $n = -5$ and $n = -7$ as two illustrative cases. These two cases are interesting as they correspond to a Harrison-Peebles-Yu-Zel'dovich scale-invariant spectrum result for the C_l 's and D_l 's, and to a possible inflation model primordial vorticity field perturbation spectrum, respectively. These two cases also span the range of constraints that can be placed on B using this method, in the range $-3 \geq n \geq -7$, i.e., $n = -5$ gives the weakest and $n = -7$ the strongest constraint on B . With $k_D \eta_0 \sim 0.4 \times 10^{14}$, from eqs. (9) and (11) B is not meaningfully constrained for $n > -3$.

3. Analysis and results

We use the foreground cleaned Q, V, and, W band co-added WMAP data (Bennett et al. 2003a) to determine the off-diagonal correlations. The data are available in the Healpix format (Gorski, Hivon, & Wandelt 1998b) at resolution $N_{\text{side}} = 512$. For each value of the magnetic field amplitude B we generate 5000 simulations of the CMB sky, and each time apply the $Kp2$ Galactic cut mask prior to computing the model D_l 's. The expected value of the model D_l 's, obtained from the mean of these simulations, is then compared with the D_l 's obtained similarly from the WMAP data, using the χ^2 statistic. Confidence levels on the field strength are derived from the resulting likelihood function.

Specifically, each simulation is a realization of the CMB with power spectrum C_l given by the best fit flat- Λ CDM model with power-law primordial power spectrum (Spergel et al. 2003), and with D_l the same as that predicted by eq. (10) (or more specifically eqs. [14] or [15]) for a given value of B . In other words, we generate a_{lm} 's such that they satisfy

$$\langle a_{lm}^* a_{l'm'} \rangle = \delta_{m,m'} [\delta_{l,l'} C_l + (\delta_{l+1,l'-1} + \delta_{l-1,l'+1}) \overline{D}_l], \quad (16)$$

instead of

$$\langle a_{lm}^* a_{l'm'} \rangle = \delta_{m,m'} \delta_{l,l'} C_l. \quad (17)$$

The a_{lm} 's are generated upto an l_{\max} of 512 (corresponding to Healpix resolution $N_{\text{side}} = 256$; since the WMAP data are expected to contain useful cosmological information upto such an l_{\max}). These are then convolved with the beam functions of each of the Q, V, and W radiometer channels (8 in all) to produce 8 maps at Healpix resolution $N_{\text{side}} = 512$ (because the noise maps have this resolution). Independent Gaussian noise realizations of rms $\sigma_0/\sqrt{N_{\text{obs}}}$ from WMAP are added to the maps, and the 8 maps are co-added weighted by $N_{\text{obs}}/\sigma_0^2$, where the effective number of observations N_{obs} varies across the sky, and σ_0 is different for each radiometer channel. This is how each simulation is created. Hereafter the same analysis procedure that is applied to the data map is applied to each of the simulations. This consists of bringing the co-added map down to Healpix resolution $N_{\text{side}} = 256$ (since we mostly use D_l 's only upto an l_{\max} of 300 in the subsequent analysis), and applying the $Kp2$ sky cut prior to computing the D_l 's.

The whole analysis can be repeated for different values of the spectral index n that characterizes the spectrum of the magnetic field perturbations.

Fig. 1 shows the D_l 's obtained from the WMAP data (crosses) and the median and 68% confidence range contours from simulations for two illustrative values of B . The spread of about 10^{-3} mK² in the 68% confidence contours for $l(l+1)D_l$ is consistent with what is expected from cosmic variance alone.

To compare the likelihoods for different B values, we use the diagonal χ^2 statistic

$$\chi^2 = \sum_{l=2}^{300} \frac{(D_l^W - \overline{D^S}_l)^2}{\sigma_l^2}, \quad (18)$$

where D_l^W is the WMAP data value, and $\overline{D^S}_l$ the average and σ_l the standard deviation of the D^S_l , both obtained from 5000 model simulations, for each value of B . Note that we do not use the full covariance matrix for the D_l 's but rather just the diagonal terms. This is because 5000 simulations are not sufficient to produce a reliably converged full covariance matrix for the D_l 's. As also noted by Eriksen et al. (2004b), for example, even the above

χ^2 test can provide a just comparison between data and simulations. The likelihood is proportional to $e^{-\chi^2/2}$. We calculate the likelihood for a few different values of B .

The likelihood function obtained for the $n = -5$ case is shown in Fig. 2. After integration, we get a 3σ confidence upper limit of $B < 15$ nG. As we can see from Fig. 2, $B=0$ G, which corresponds to pure Gaussian primordial fluctuations, is within the 1σ confidence range from the peak of the likelihood function (this 1σ range corresponds to a δB of 3.9 nG). The jaggedness in the likelihood function is from the fluctuation of mean D_l 's used in calculating χ^2 (see Fig. 1). With 5000 simulations, the fluctuation of mean D_l 's should be of the order of $\sigma_l/\sqrt{5000}$. This results in a fluctuation of 0.1 in the χ^2 values, or a 5% uncertainty in the estimated likelihood. This does not much affect the results of our analysis (for example for the 3σ limit on B we look for a $\Delta\chi^2$ of 9, which is not very sensitive to a 5% uncertainty in the estimated likelihoods).

For the $n = -7$ case (see Fig. 3), the 3σ confidence limit is $B < 1.7$ nG, and again the pure Gaussian primordial fluctuation case with $B = 0$ G is not far from the 1σ confidence range from the peak. In this case 1σ corresponds to a $\delta B = 0.4$ nG. More stringent limits are obtained in this case as expected (eq. [15] shows that larger D_l 's with a stronger l -dependence are predicted by the model for $n = -7$).

The conditions of homogeneity and unidirectionality of the primordial magnetic field may be a better approximation on some scales rather than others. In each of the above cases for n , other ranges in l , such as $2 - 100$, $101 - 200$, $201 - 300$, or $2 - 500$, did not indicate anything qualitatively different, i.e., $B = 0$ G remains a satisfactory fit.

4. Conclusions

We study off-diagonal correlations of the form $D_l = \overline{\langle a_{l-1,m} a_{l+1,m}^* \rangle}$ in the first year WMAP CMB anisotropy data. Such correlations can result from a homogeneous primordial magnetic field. We do not find significant off-diagonal correlations in the data, which appear to be satisfactorily fit by a zero primordial magnetic field hypothesis. We place 3σ upper limits on the strength of the magnetic field of $B < 15$ nG for spectral index $n = -5$ and $B < 1.7$ nG for $n = -7$. These two cases are interesting as they correspond to a Harrison-Peebles-Yu-Zel'dovich scale-invariant spectrum result for the C_l 's and D_l 's, and to a possible inflation model primordial magnetic field perturbation spectrum, respectively. These two cases also span the range of constraints that can be placed on B using this method. Future CMB anisotropy data should allow for tighter constraints on a primordial cosmological magnetic field.

We acknowledge useful discussions with R. Durrer and A. Kosowsky. GC, TK, and BR acknowledge support from NSF CAREER grant AST-9875031 and DOE EPSCoR grant DE-FG02-00ER45824. TK also acknowledges CRDF-GRDF grant 3316. PM and YW acknowledge support from NSF CAREER grant AST-0094335.

REFERENCES

- Adams, J., Danielsson, U. H., Grasso, D., & Rubinstein, H. 1996, *Phys. Lett. B*, 388, 253
- Bamba, K., & Yokoyama, J. 2004, *Phys. Rev. D*, 69, 043507
- Bennett, C. L., et al. 2003a, *ApJS*, 148, 1
- Bennett, C. L., et al. 2003b, *ApJS*, 148, 97
- Bershadskii, A., & Sreenivasan, K. R. 2004, *astro-ph/0403702*
- Chiang, L.-Y., Naselsky, P. D., Verkhodanov, O. V., & Way, M. J. 2003, *ApJ*, 590, L65
- Coles, P., Dineen, P., Earl, J., & Wright, D. 2004, *MNRAS*, in press, *astro-ph/0310252*
- Colley, W. N., & Gott, J. R. 2003, *MNRAS*, 344, 686
- Colley, W. N., Gott, J. R., & Park, J. R. 1996, *MNRAS*, 281, L82
- Copi, C. J., Huterer, D., & Starkman, G. D. 2003, *astro-ph/0310511*
- de Oliveira-Costa, A., Tegmark, M., Davies, R. D., Gutierrez, C. M., Lasenby, A. N., Rebolo, R., & Watson, R. A. 2003, *astro-ph/0312039*
- Durrer, R., Kahniashvili, T., & Yates, A. 1998, *Phys. Rev. D*, 58, 123004 (DKY)
- Eriksen, H. K., Hansen, F. K., Banday, A. J., Górski, K. M., & Lilje, P. B. 2004a, *ApJ*, in press, *astro-ph/0307507*
- Eriksen, H. K., Novikov, D. I., Lilje, P. B., Banday, A. J., Górski, K. M. 2004b, *astro-ph/0401276*
- Fischler, W., Ratra, B., & Susskind, L. 1985, *Nucl. Phys. B*, 259, 730
- Giovannini, M. 2003, *astro-ph/0312614*
- Giovannini, M., & Shaposhnikov, M. 1998, *Phys. Rev. Lett.*, 80, 22

- Górski, K. M., Hivon, E., & Wandelt, B. D. 1998b, in *Evolution of Large-Scale Structure: From Recombination to Garching*, ed. A. J. Banday, R. K. Sheth, & L. A. N. da Costa (Enschede: Print Partners Iskamp), 37
- Górski, K. M., Ratra, B., Stompor, R., Sugiyama, N., & Banday, A. J. 1998a, *ApJS*, 114, 1
- Gurzadyan, V. G., et al. 2004, astro-ph/0402399
- Hajian, A. & Souradeep, T. 2003, *ApJ*, 597, L5
- Hansen, F. K., Cabella, P., Marinucci, D., & Vittorio, N. 2004, astro-ph/0402396
- Komatsu, E., et al. 2003, *ApJS*, 148, 119
- Kulsrud, R. M. 1999, *Ann. Rev. Astron. Astrophys.*, 37, 37
- Lewis, A. 2004, astro-ph/0403583
- Mack, A., Kahniashvili, T., & Kosowsky, A. 2002, *Phys. Rev. D*, 65, 123004
- Mukherjee, P., Coble, K., Dragovan, M., Ganga, K., Kovac, J., Ratra, B., & Souradeep, T. 2003, *ApJ*, 592, 692
- Mukherjee, P., Dennison, B., Ratra, B., Simonetti, J. H., Ganga, K., & Hamilton, J.-Ch. 2002, *ApJ*, 579, 83
- Mukherjee, P., Hobson, M. P., & Lasenby, A. N. 2000, *MNRAS*, 318, 1157
- Mukherjee, P., & Wang, Y. 2004, astro-ph/0402602
- Park, C.-G. 2004, *MNRAS*, 349, 313
- Park, C.-G., Park, C., & Ratra, B. 2002, *ApJ*, 568, 9
- Park, C.-G., Park, C., Ratra, B., & Tegmark, M. 2001, *ApJ*, 556, 582
- Peebles, P. J. E. 1980, *The Large-Scale Structure of the Universe* (Princeton: Princeton University Press), 356
- Peebles, P. J. E., & Ratra, B. 2003, *Rev. Mod. Phys.*, 75, 559
- Pogosian, L., Vachaspati, T., & Winitzki, S. 2002, *Phys. Rev. D*, 65, 083502
- Ratra, B. 1985, *Phys. Rev. D*, 31, 1931
- Ratra, B. 1992, *ApJ*, 391, L1

- Semikoz, V. B., & Sokoloff, D. D. 2004, *Phys. Rev. Lett.*, 92, 131301
- Seshadri, T. R., & Subramanian, K. 2001, *Phys. Rev. Lett.*, 87, 101301
- Sigl, G., Olinto, A. V., & Jedamzik, K. 1997, *Phys. Rev. D*, 55, 4582
- Spergel, D., et al. 2003, *ApJS*, 148, 175
- Subramanian, K., Seshadri, T. R., & Barrow, J. D. 2003, *MNRAS*, 344, L31
- Tegmark, M., de Oliveira-Costa, A., & Hamilton, A. J. S. 2003, *Phys. Rev. D*, 68, 123523
- Vachaspati, T. 1991, *Phys. Lett. B*, 265, 258
- Vielva, P., Martínez-González, E., Barreiro, R. B., Sanz, J. L., & Cayón, L. 2004, *ApJ*, in press, astro-ph/0310273
- Widrow, L. A. 2002, *Rev. Mod. Phys.*, 74, 775

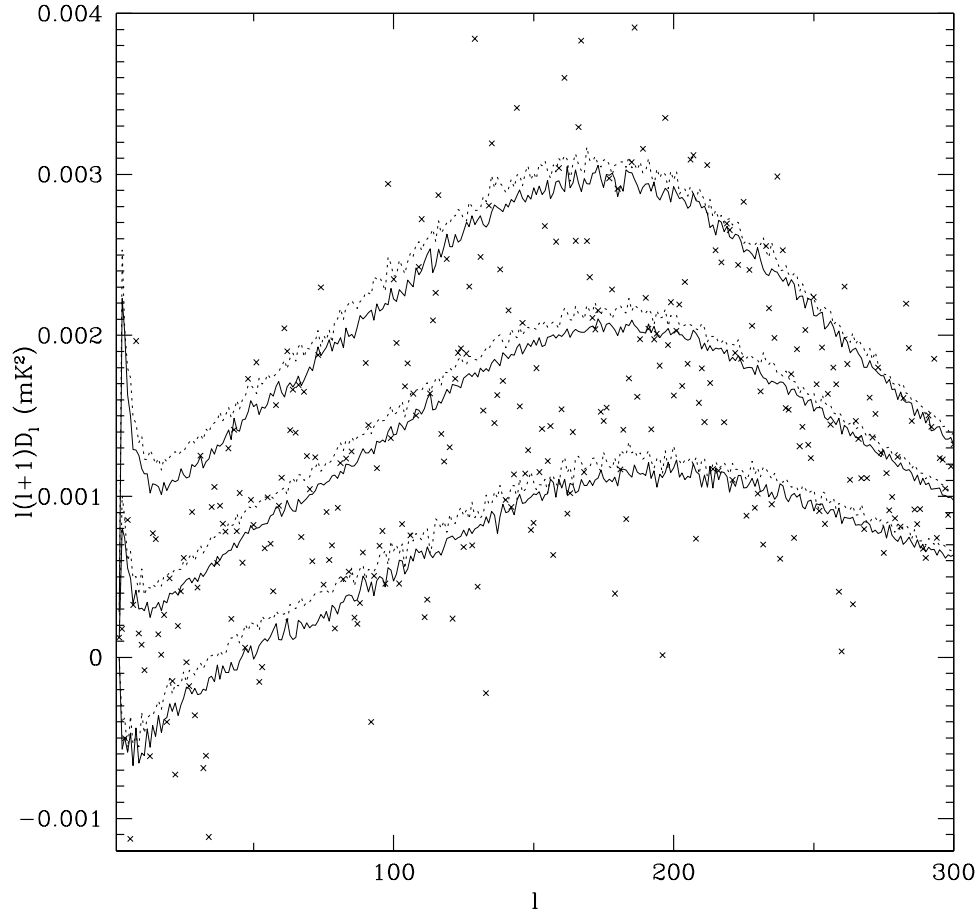


Fig. 1.— Off-diagonal power spectra obtained from the WMAP data (crosses) and the median and 68% confidence contours obtained from model simulations with magnetic field strengths $B = 0$ (solid lines) and 16 (dotted lines) nG, for a magnetic field perturbation spectral index $n = -5$.

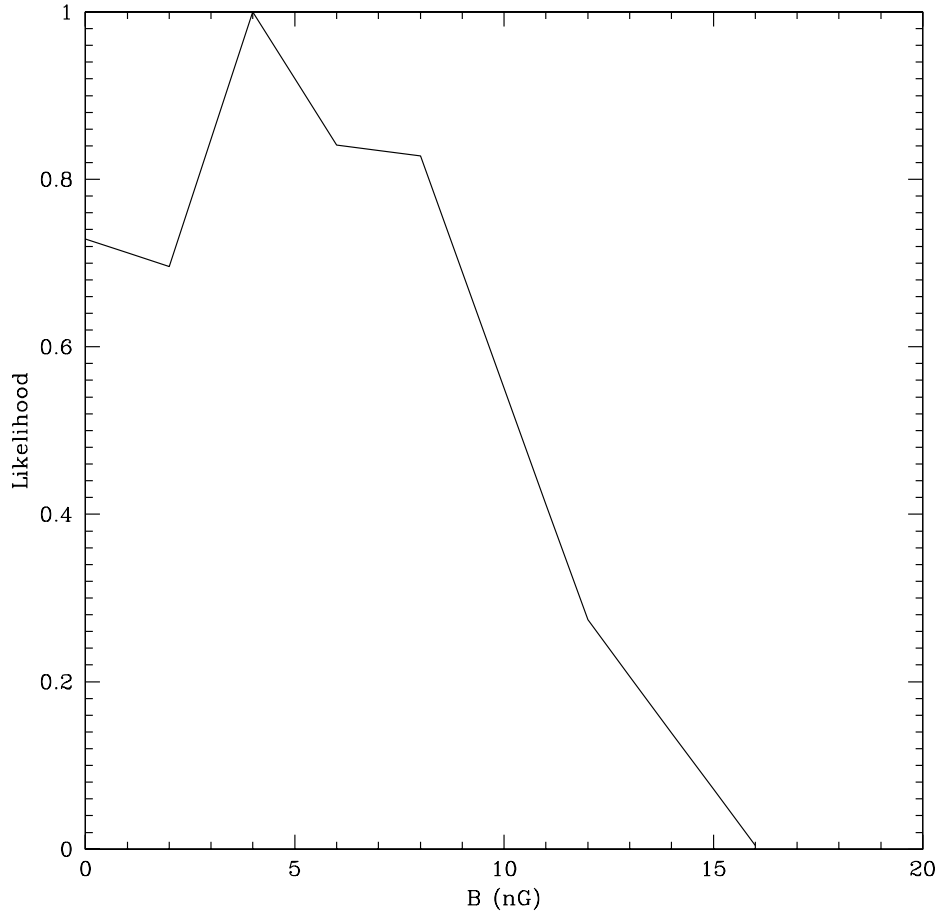


Fig. 2.— The likelihood as a function of the strength of the magnetic field for a magnetic field perturbation spectral index $n = -5$.

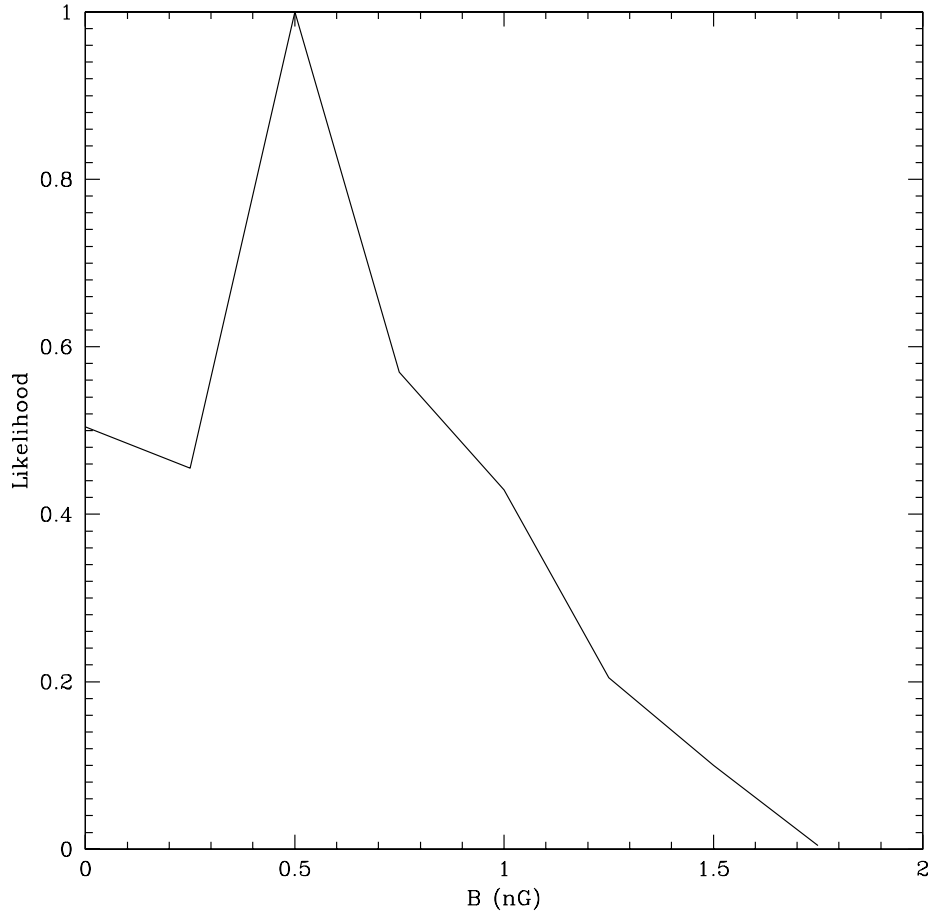


Fig. 3.— The likelihood as a function of the strength of the magnetic field for a magnetic field perturbation spectral index $n = -7$.